



Shape fabrics of particles in low concentration suspensions: 2D analogue experiments and application to tiling in magma

LAURENT ARBARET and HERVÉ DIOT

Université Blaise-Pascal, CNRS URA no 10, 5 rue Kessler, 63038 Clermont-Ferrand, France

and

JEAN-LUC BOUCHEZ

Université Paul-Sabatier, CNRS URA no 67, Laboratoire de Pétrophysique et Tectonique, 38 rue des
 Trente-Six Ponts, 31400 Toulouse, France

(Received 23 August 1995; accepted in revised form 22 January 1996)

Abstract—Jeffery's equations ascribe a theoretical cyclic nature to the shape fabric of non-interacting rigid particles immersed in a viscous fluid undergoing simple shear flow. This theoretical behaviour is confirmed at 'low' shear strains ($\gamma < 6$) by two-dimensional experiments in a torsion apparatus, inducing shape fabric development of particles evenly distributed on the surface of a silicon fluid and at low particle concentrations (13–14% in area). For larger shear strains however ($6 < \gamma < 20$), the shape fabric orientation tends to remain close to the shear plane, its magnitude remains at low values and the cyclicity of the fabric disappears. This is due to interactions between particles, forming tiling features with variable shape ratios. Interactions rapidly increase in number for $\gamma > 5$ (first experiment: 134 identical particles) or $\gamma > 1$ (second experiment: 178 particles with two size classes), then become stable at 17% (first experiment) and at more than 50% (second experiment) of the population of particles. Due to the contribution of the tiled particles, the shape fabric becomes asymmetrical in its orientation distribution, with a maximum lying above the shear plane. The latter result provides a new shear sense indicator, in addition to the statistical determination of the tiled features. The study also suggests that crystalline fabrics in magmas could be acquired at high melt fractions, i.e. early in the crystallization history of the magma. Copyright © 1996 Elsevier Science Ltd

INTRODUCTION

Shear sense determination in plastically deformed rocks plays an important role in its kinematic integration into large geological systems. This problem is generally addressed using two types of criteria (Choukroune *et al.* 1987), namely (1) strain features derived from some kind of heterogeneity during progressive strain, such as drag folds, asymmetrical objects, etc., and (2) obliquities between the imposed kinematic framework (shear plane and direction) and other frameworks (lattice fabric, shape fabric, finite strain ellipsoid axes, etc.). In magmas, the mineral foliation and associated lineation are, for the sake of simplicity, usually equated directly to the kinematic framework to model the geometry of the flow during emplacement of a body (Nicolas 1992). However, sense of shear determination remains a major goal and is usually deduced from both types of criteria: (i) analysis of the tiling of crystals (Blanchard *et al.* 1979, Blumenfeld 1983, Blumenfeld & Bouchez 1988, Paterson *et al.* 1989), and (ii) obliquity between fabrics of crystal populations having different aspect ratios (Fernandez *et al.* 1983, Benn & Allard 1989).

The first criterion statistically establishes the sense of shear from the preferred sense of tiling of crystals, such as K-feldspar megacrysts in a porphyritic granite. However, the mode of formation and the evolution of

tiled particles still have to be better understood, and this paper contributes to this goal. For the second criterion, which is based on the average rotation rates of sub-fabric ellipsoids (see below), it is not yet clear whether such subfabrics can be initiated at low concentrations and for large shear strains.

The theoretical analysis and experimental study of preferred directional orientation, or shape fabric, developed by rigid markers immersed in a viscous fluid deformed by homogeneous simple shear are described by the equations of Jeffery (1922), which give the rotation of a rigid ellipsoid. The rotation of bodies having simple shapes, such as cylinders or parallelepipeds, has been experimentally evaluated by Willis (1977). In two-dimensions, similar conclusions have been presented experimentally and numerically by Fernandez *et al.* (1983) for rectangular markers. For irregular shapes however, Willis (1977) observed that the rotation of particles may not be described accurately by the rotation model of Jeffery (1922). A typical deviation from the theoretical rotation model comes from the clustering of crystals. The piling up of crystals like tiles on a roof, first invoked by Den Tex (1969), constitutes the simplest form of mechanical interaction between particles. Tiling of K-feldspar phenocrysts in a granite has been reported and interpreted by Blumenfeld (1983) in the Barbey-Seroux granitic body. It has been experimentally reproduced by

Fernandez *et al.* (1983) using rigid particles in simple shear flow with shear strain values ranging from $\gamma = 3$ to $\gamma = 5$.

In concentrated suspensions, the consequence of interactions between particles on the development of a two-dimensional shape fabric is important. In simple shear flow, these interactions will annihilate the cyclic evolution of the fabric (see below). Consequently, for high shear strains ($\gamma > 3$), the fabric long-axis remains close to the shear plane (Ildefonse *et al.* 1992b).

In low concentration suspensions, i.e. without substantial interactions, the development of a shape fabric is theoretically cyclic (Fig. 1a). With increasing shear strain, the shape fabric long-axis rotates at a rate which depends on the aspect ratio of the particles. In simple shear, the integration of the equation giving the general motion of a particle (Willis, 1977) yields the critical shear strain γ_T (Fig. 1b) corresponding to one complete rotation of the particle (Fernandez *et al.* 1983):

$$\gamma_T = \frac{4\pi}{\sqrt{1-K^2}}, \quad \text{with} \quad K = \frac{n^2-1}{n^2+1};$$

where n is the aspect ratio of the particle. γ_T also characterises the critical shear strain (Fig. 1b) of the fabric for a population of particles provided that the particles do not interact and have identical shapes. For such a population, both the angle α between the long-axis of the fabric ellipse and the shear direction defined with positive or negative values with respect to the sense of shear (Fig. 1c), and the fabric intensity D , evolve cyclically (Fig. 1a). D reaches a maximum value of $D = n^2$ when $\alpha = 0$, i.e. when the fabric is parallel to the

shear direction, and a minimum value of $D = 1$ for $\alpha \pm 45^\circ$, corresponding to the isotropic stages of the shape fabric (Ildefonse *et al.* 1992a).

In the case of large simple shear strain, interactions between particles may become important even in low-concentration suspensions. Due to the increasing probability of contacts between particles, their clustering leads to the tiling of two or more particles (Blumenfeld & Bouchez 1988, Tikoff & Teyssier 1994). Unlike the concentrated suspensions, where the particles rapidly cease their rotation, the clusters themselves may continue to evolve cyclically. In the 2D experimental work, we discuss here the case of low concentration suspensions undergoing simple shear within a large strain domain, to understand the interaction between particles and their role on the acquisition and evolution with strain of grain shape fabrics. Thus, this paper investigates experimentally the motion of these elementary clusters, made of pairs of particles having varying aspect ratios. Departures in angular velocities of these elementary clusters from the model of Jeffery (1922) will be described and discussed, and their consequences in terms of fabrics in magmas will be stressed.

APPARATUS AND MATERIAL

Experiments were conducted in a coaxial-cylinder viscosimeter constructed in Poly Vinyl Chloride (PVC) and aluminium (Fig. 2) similar to the torsion apparatus of Passchier & Sokoutis (1993). Two counter-rotating cylinders allow experiments to be run for homogeneous shear strains as large as $\gamma = 20$. The viscous fluid is made of the pink silicon bouncing putty 'Silbione 70009' of Rhône-Poulenc, France, whose viscosity is 2.9×10^4 Pa.s at 20°C (Weijermars 1986). The applied constant linear velocity on the rotor surfaces at contact with the fluid, corresponding to $13.2^\circ \times 10^{-3} \text{ s}^{-1}$ and $20.7^\circ \times 10^{-3} \text{ s}^{-1}$ for the internal and external cylinders, yields a shear strain rate of $\dot{\gamma} = 4 \times 10^{-4} \text{ s}^{-1}$ in the fluid. At this rate, the flow behaviour of the putty is Newtonian (Passchier & Sokoutis 1993). Rectangular rigid markers made of a composite aluminium-cardboard sheet, 0.5 mm thick, 5–6 mm long and 2–6 mm wide, were disposed flush with the upper surface of the silicon matrix. It has been verified that the particle fluid interface was coherent, an important requirement for the particle rotation to be close to theory (Ildefonse & Mancktelow 1993). The fluid was covered with dark coloured powder ($\phi < 100 \mu\text{m}$) allowing the behaviour of the fluid around the particles during experiments to be traced. Measurements of the orientations of the particles have been performed using a numerical direction 'finder' (precision better than 1°), coupled with a computer, which calculated the orientation α of the major axis of the shape fabric ellipse, and its intensity D . Two runs of experiment were performed using a unimodal or bimodal aspect ratio of particles in order to verify if the final shape fabric can retain the memory of the initial distribution.

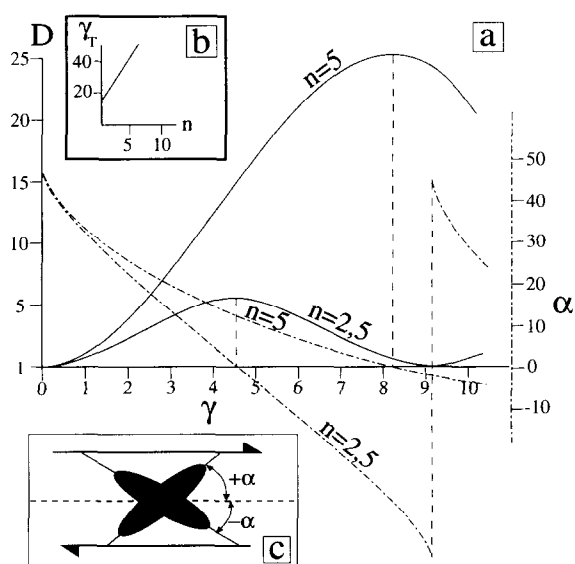


Fig. 1. (a) Theoretical curves for simple shear flow, giving the fabric intensity (maximum intensity D , solid lines) and fabric orientation (α ; dash-dot lines) as a function of the shear strain (γ) for populations of rigid particles of aspect ratios $n = 2.5$ and $n = 5$. (b) Critical shear strain γ_T as a function of n (from Ildefonse *et al.* 1992a). (c) Position of α angle with respect to the shear axis and the sense of shear.

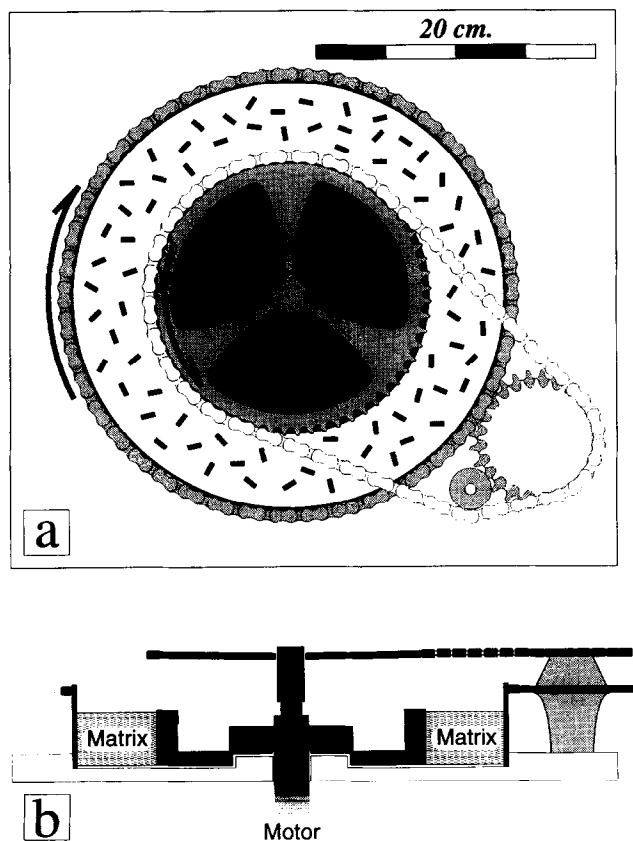


Fig. 2. Sketch of the shear apparatus. (a) The inner cylinder is driven by an electric motor with reduction gears. A chain-sprocket system drives the outer cylinder in the opposite direction with an equal angular speed relative to the inner cylinder (0.038 mms^{-1} at the surface in contact with the silicone). (b) Cross-section of the viscosimeter. The base of the box is covered by liquid soap lubricant which minimises friction against the lower immobile surface and the silicone putty. The remainder of the box is filled with silicone putty ($< 4 \text{ cm}$ thick). The particles are introduced flush with the surface of the bubble-free silicon.

EXPERIMENTAL RESULTS

First experiment: unimodal shape fabric

The development of shape-preferred orientations in a low-concentration suspension of identical particles was tested for shear strains up to $\gamma = 20$. One hundred and thirty-four particles, with aspect ratio $n = 2.5$ and covering 12.8% of the total area, were evenly distributed on the surface of the silicon matrix. Their initial orientation distribution (Fig. 3) yields a fabric axis at $\alpha_0 = -25^\circ$, with an intensity $D_0 = 1.17$, that is very close to random.

As soon as $\gamma = 1$, the shape fabric orientation is already closely comparable to theory (Fig. 3). For $1 < \gamma < 4$, the particles rotate without interactions (Fig. 3; $\text{IP}\% = 0$), and the corresponding fabrics evolve according to the model of Jeffery. At $\gamma = 4$, the first interaction is observed, with the tiling of two particles. At $\gamma = 6$, the first substantial discrepancy from theory is observed: the fabric long-axis gets closer to the shear plane than predicted. This behaviour reflects the increasing percentage of interacting particles: $\text{IP}\% = 3\%$ at $\gamma = 5$ and

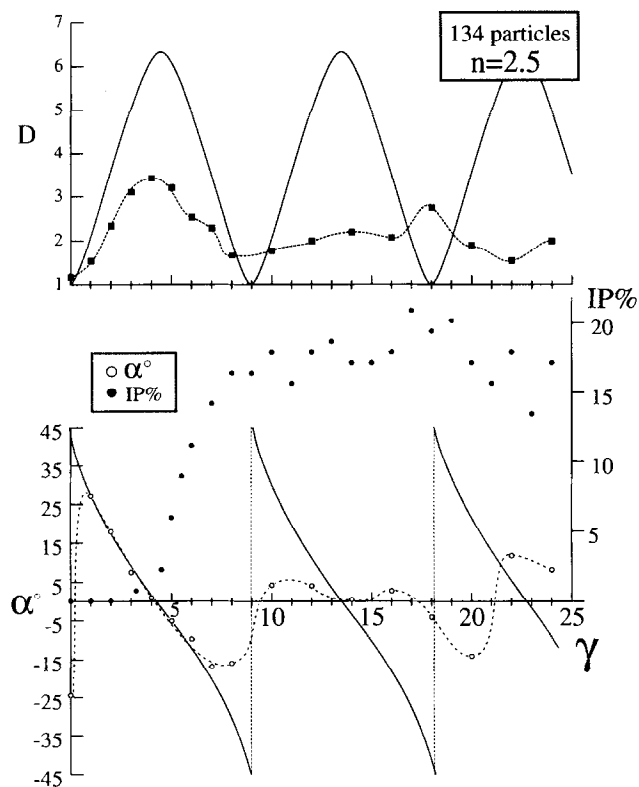


Fig. 3. Evolution with shear strain γ of the intensity D (upper diagram) and orientation α (lower diagram) of the shape fabric of 134 particles with axial ratio $n = 2.5$. Symbols along dashed lines are experimental data; solid lines are theoretical curves. Filled circles give the percentage of interacting particles ($\text{IP}\%$).

$\text{IP}\% = 14\%$ at $\gamma = 7$. For $\gamma > 7$, the behaviour of α departs completely from theory. At the same time, the percentage of interacting particles increases and reaches 17% at $\gamma = 10$. For $\gamma > 10$, the percentage of interactions remains stable, or even tends to decrease for $\gamma > 17$, due to the cyclic nature of tiling, with particles in contact replaced by particles separating from each other after a given amount of common rotation. The observed interacting particles are mostly composed of pairs of particles. Only three aggregates of three particles, representing 2.2% of the population in area, have been observed between $\gamma = 10$ and $\gamma = 18$.

Second experiment: bimodal shape fabric

Two different populations of 89 particles each have been used, with aspect ratios $n_1 = 2.5$ and $n_2 = 3.3$, and covering 14.8% of the total area (Fig. 4). In the following, the fabric of each population, or subfabric, is described separately; the total fabric is then presented.

As in the first experiment, the shape fabric of each population of particles evolves according to the model of Jeffery (1922) for $1 < \gamma < 6$ (Figs. 5a & b). For higher shear strains ($\gamma > 7$), both subfabrics show important discrepancies in the behaviour of α and D with respect to theory, although they tend to follow the same cyclic bulk variation. A comparison between the subfabrics shows

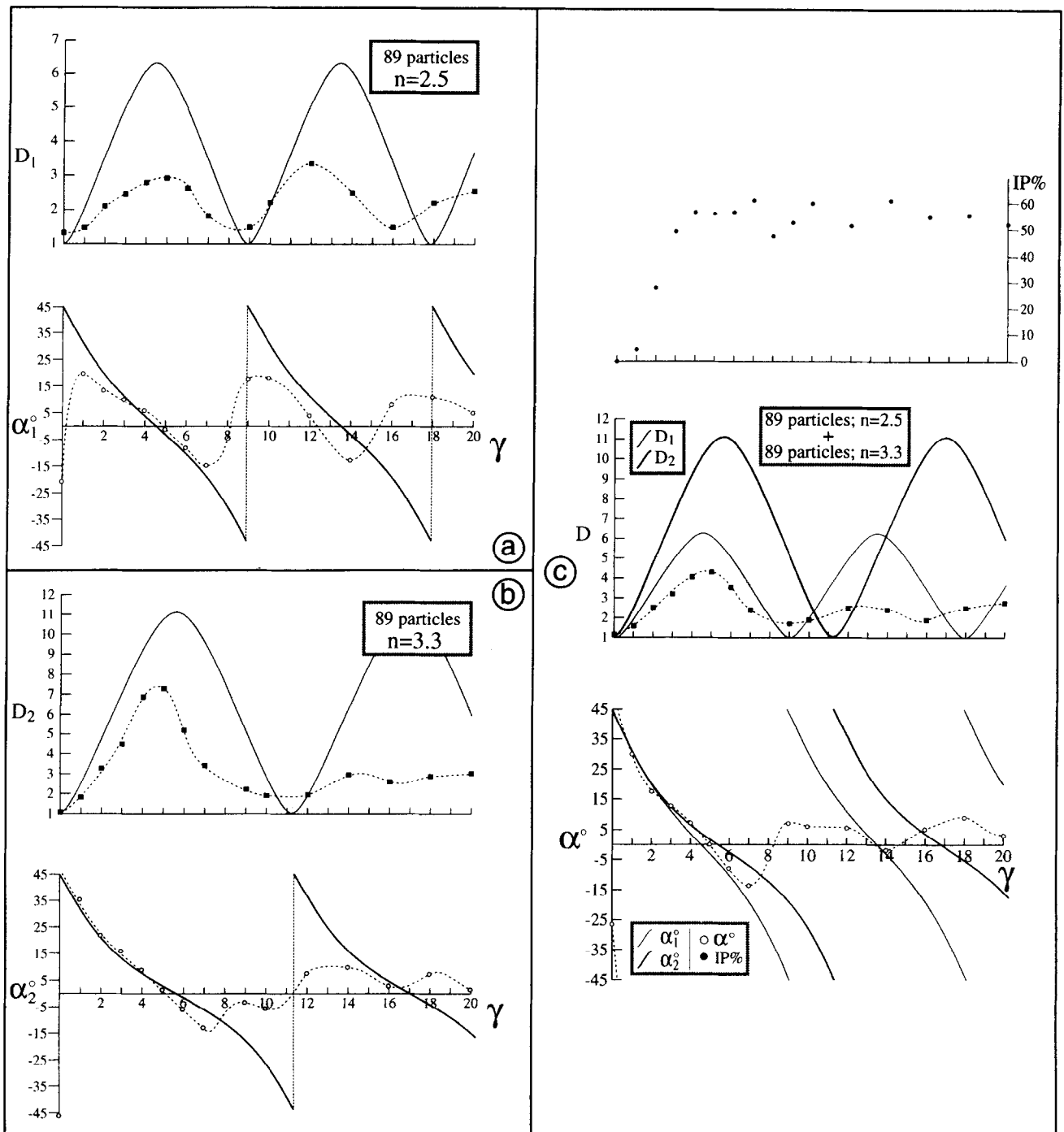


Fig. 5. (a) Evolution with shear strain γ of the intensity D_1 (upper diagram) and orientation α_1 of the shape fabric of 89 particles with axial ratio $n_1 = 2.5$ compared to the theoretical curve (continuous line) for the same aspect ratio. Symbols along dashed lines are experimental data; solid lines are theoretical curves. (b) Same as (a) but with axial ratio $n_2 = 3.3$. (c) Evolution with γ of the intensity D and orientation α of the shape fabric of the total population of particles. Solid lines: theoretical curves. Filled circles give the percentage of interacting particles (IP%).

that the fabric orientation of the shortest particles experiences larger variations around the shear plane ($\alpha_1 = +20$ to -15°) than do the longest particles ($\alpha_2 = +10$ to -5°). The fabric intensity D_1 is observed to evolve cyclically up to the highest shear strains but with much lower magnitudes than for theory (Fig. 5a). By contrast, D_2 is cyclic only during the first theoretical cycle; then, for $\gamma > 6$, D_2 tends to stabilise with a mean intensity of about 3 (Fig. 5b).

Studying the two populations together, the mean α

and D of the total fabric display only a hint of memory of the cyclicity expected from theory (Fig. 5c). Note that, even before the first cycle is completed, α tends to remain above the shear plane.

In this second experiment, interacting particles appear as soon as $\gamma = 1$ and their percentage increases rapidly up to 55% for $\gamma > 4$ (Fig. 5c). This percentage is larger than in the first experiment. This result is due not only to the relative increase in the area occupied by the particles (14.8 against 12.8%), but rather to the increase in the

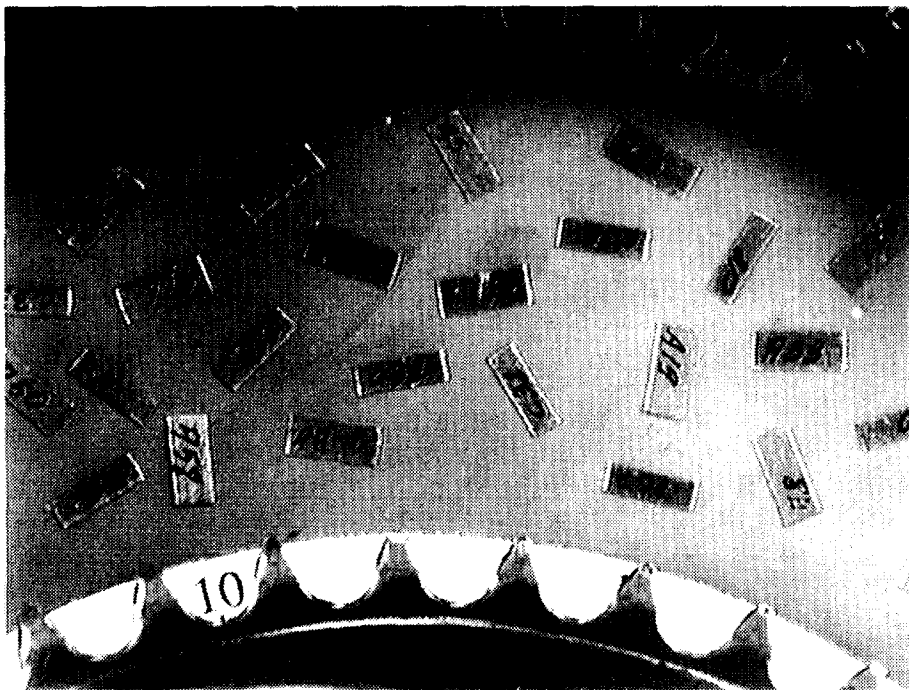


Fig. 4. Initial stage ($\gamma = 0$) of the second experiment with two different populations of particles covering 14.8% of the total area.

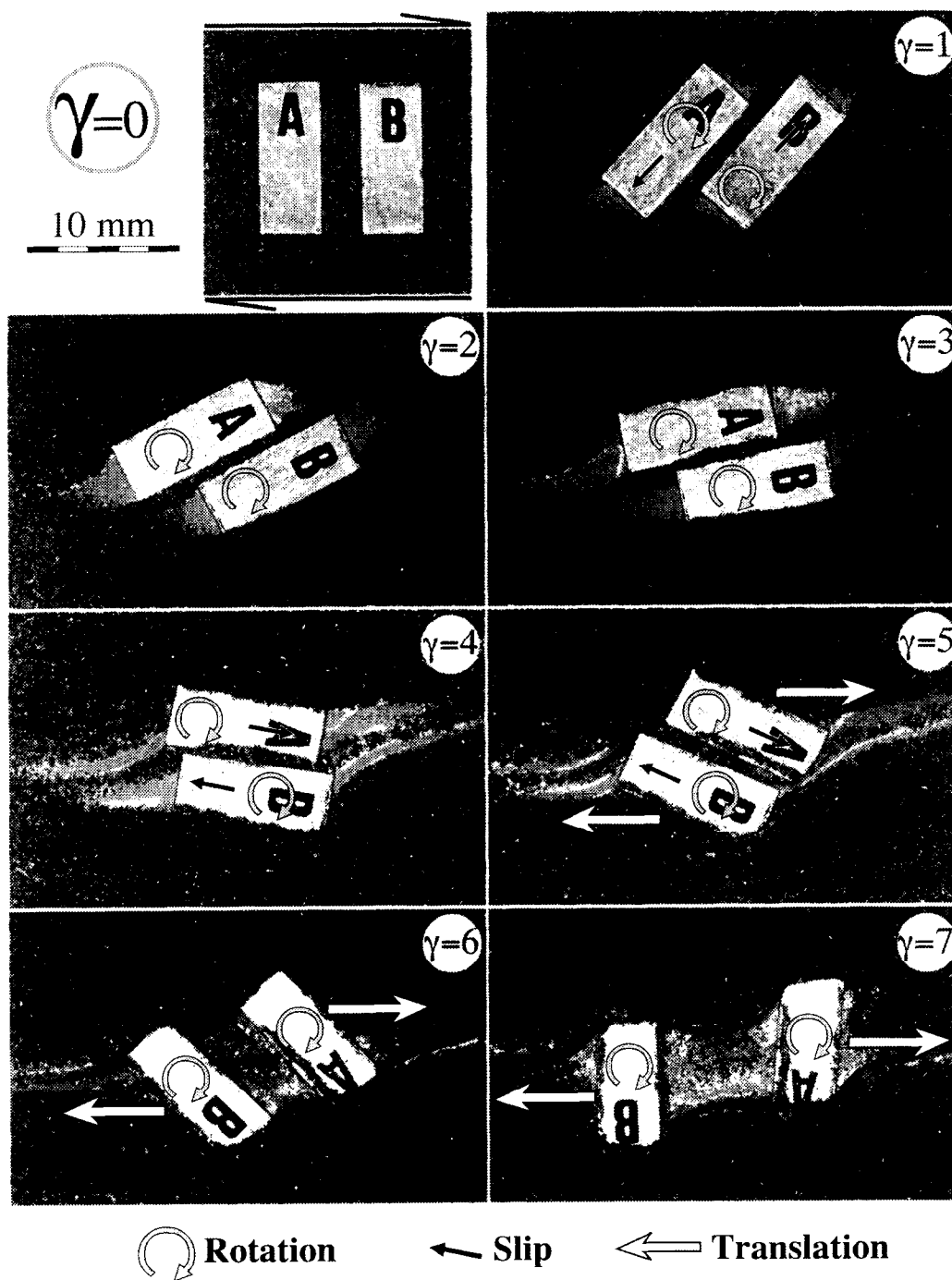


Fig. 6. Example of development of tiling in the case of two particles having an aspect ratio $n = 2.5$ (10 mm long and 4 mm wide) in a dextral simple shear flow for $\gamma = 1$ to 7.

number of particles (178 against 134). In spite of this high frequency of interactions, they do not substantially disturb the evolution of the shape fabric up to $\gamma < 6$, which remains principally controlled by the rotation of the particles. For larger γ values, the effect of interactions on the shape fabric becomes dominant. The particles tend to form clusters with up to 9 particles within a cluster, representing up to 12% of the population by number, but these clusters are particularly unstable. Hence, as in the first experiment, most clusters are composed of two particles, and this observation is independent of the amount of shear strain.

Conclusion from the experiments

Summarising the results of our experiments, the shape ratio variations of the particles and the tiling of particles are identified as the two factors that affect $D(\gamma)$ and $\alpha(\gamma)$. Fabrics of isolated, rectangular particles are relatively simple to understand since, whatever the particles variations in aspect ratios, their rotation is given by the model of Jeffery (1922), and hence $D(\gamma)$ and $\alpha(\gamma)$ are readily predictable. However, even in low concentration suspensions, particle interactions occur, principally in the form of tiling. Fabrics of tiled particles are more complex since the objects have (i) complex shapes, and (ii) various aspect ratios depending on their overlap during rotation. Both factors contribute to the observed strong variations in the resulting fabrics.

In the following, and for simplicity, only pairs of identical particles are studied experimentally, and compared with the behaviour of single particles. First, the formation, rotation, and disruption of a tiled aggregate are explored, then the rotation behaviour of tiled particles will be examined as a function of their aspect ratios

THE TILING PHENOMENON

General evolution and shear sense indication

Tiling occurs when two particles reach a side-by-side configuration (Fig. 6). Three stages characterise the evolution of tiling (Launeau & Bouchez 1992): initiation, aggregation and separation. Initiation occurs (Fig. 6: $\gamma = 1$) when two particles close enough to each other tend to get closer due to the perturbed flow in the fluid between the particles. At this stage, variations in the colour of the surface of the fluid, which has been powdered with black dust, reveals that the fluid located between the particles is compressed and ejected upward and laterally. When aggregation is achieved (Fig. 6: $\gamma = 2$), the pair of particles undergoes a common rotation. Two time periods characterise this aggregation–rotation stage (Fig. 7). The first period corresponds to the time during which α is positive, i.e. the orientation of the particles is above the shear axis. During this period of time, the angular velocity is slightly lower than the

theoretical one for a single particle. The second stage is characterised by the abrupt acceleration of the angular velocity of the pair of particles when α becomes negative, i.e. when the orientation of the particles passes through the shear plane. Note that during this stage the angular velocity remains higher than the theoretical one for a single particle. Note also that during this aggregation time, no substantial slip between the particles past each other is observed except just before separation (Fig. 6: $\gamma = 4$). After separation, the angular velocity becomes irregular due to the flow perturbation inbetween the particles.

In terms of shear sense indication, note that, at the beginning of separation (Fig. 6; $\gamma = 5$), if the position of the particles only are considered, the tiling feature may be taken as being due to sinistral shear, whereas the imposed shear was dextral. However, in both experiments, never more than 15% of the tiling features could be taken for sinistral. This is because the time span during which the particles in contact display a sense of shear coherent with the imposed shear sense is clearly dominant compared to the time during which ‘inverse’ tiling occurs. The conclusion is that, as far as a natural magma can be compared with the present suspension, a statistically dominant sense of tiling may be used as a shear sense criterion, as postulated by Blumenfeld & Bouchez (1988).

Rotation of a pair of particles

A pair of particles is a complex system that cannot be modelled numerically; consequently the variation of its critical shear strain γ_T was studied using the torsion apparatus. Rigid 2D objects having the morphology of pairs of particles were used ($a =$ length, $b =$ width, $a \geq b$, and $L =$ ‘free length’ as shown in Fig. 8a). The results of the experiments are plotted graphically for $a = 6$, $b = a/3$, $a/2$, $2a/3$ and a with different values of L ($0 < a$, Fig. 8a). When $L = 0$, the pair of particles becomes identical to a rectangular particle with $a' = a$ and $b' = 2b$.

A general rise of the critical shear strain γ_T occurs when L increases, due to the associated increasing stability of the objects about the shear plane. However, except for $L = 0$, $\gamma_T(L)$ is not linear and a net increase of its slope is observed at about $L = b$, whatever the value of L (Fig. 8a). Another important observation from these experiments is the presence of an angle β (Fig. 8b) between the shear plane and the orientation for which the angular velocity of the tiled particles is minimum. The minimum velocity, which is the inflection point of the $\alpha(\gamma)$ curve, appears when the long axis of the pair of particles is parallel to the shear plane (Fig. 8b), as expected in terms of the maximum torque acting on the pair of particles. In this orientation, the long axis of the constituting particles, which is the reference axis for the measurement of the shape fabric, is at an angle β to the imposed shear plane and the magnitude of β decreases as L increases (Fig. 8b, box).

In these experiments, the variations in grey tones

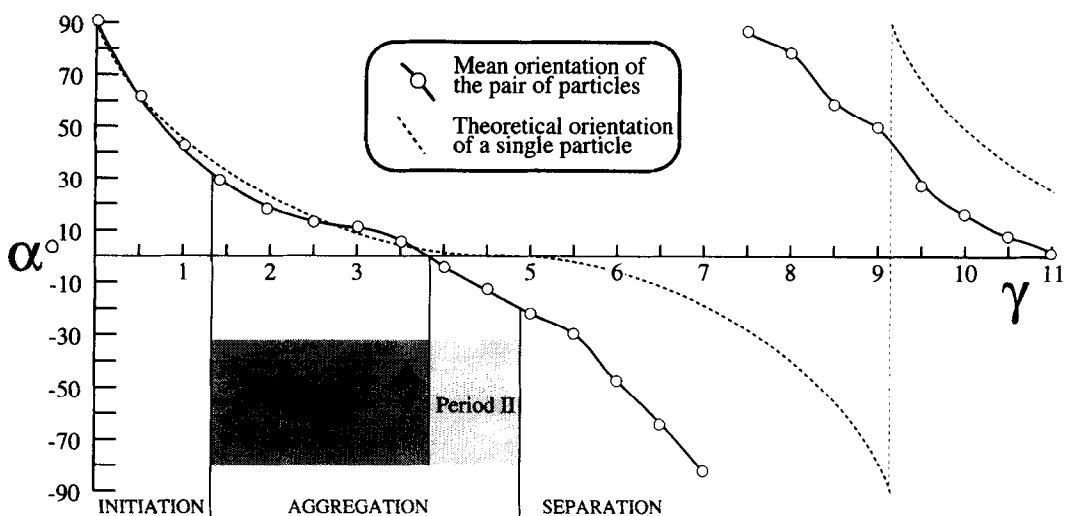


Fig. 7. Evolution with γ of the orientation of two identical particles ($n = 2.5$) during the tiling process. Dashed line: theoretical curve for a single particle with the same aspect ratio.

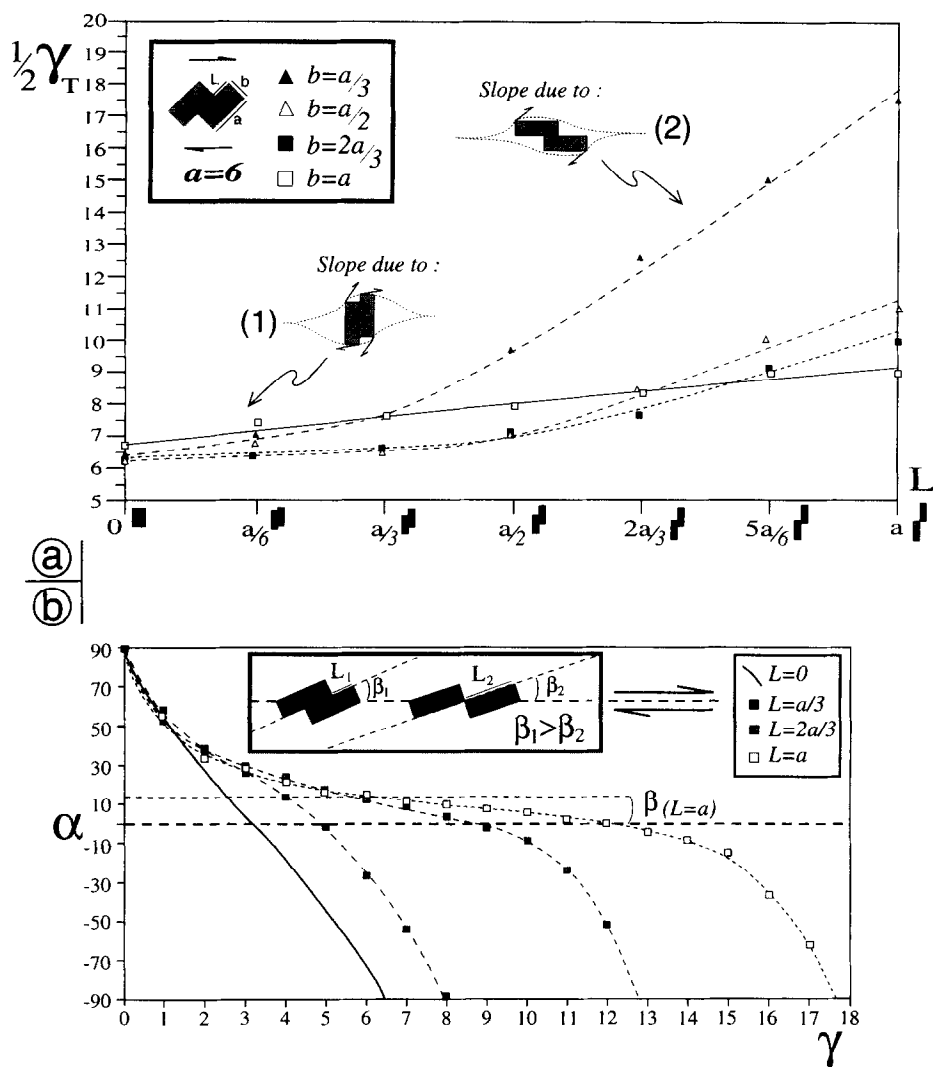


Fig. 8. (a) Variation of γ_T as a function of the 'free length' L of a pair of particles for different values of the width b of each particle. Cartoons indicate the influence of 'free length' L on the torsional forces in the case of $b = a/3$: (1) when $L < b$ and particles are perpendicular to the shear plane, torsional forces act on the two corners of the particles. For higher values of L , one corner is protected in the pressure shadow of the other and only one force appears. (2) The general increase in γ_T is due to the relative stability of the particle aggregate along the shear plane compared to a single rectangular particle. (b) Evolution of α as a function of γ for different values of L in the case of $a = 6$ and $b = a/3$. Note that the minimal angular velocity, i.e. minimum slope of the curves, is above the shear plane at β (orientation of the long axis of the pair of particles), whatever the value of L .

related to powder surface density help to visualise the flow perturbations in the fluid that may reach a distance of twice the length of a particle (Ildefonse *et al.* 1992b). Emergence of silicon putty (Fig. 6) typically represents pressure shadows like in the σ -type porphyroclasts of Passchier & Simpson (1986) and Van den Driessche & Brun (1987). These pressure shadows occur in two places (Fig. 6) at the tips of the particles, and correspond to a transtensional zone within the extensional quadrant of the flow (Hanmer 1990); along the sides of the particles they correspond to interfaces along which the fluid is dragged with the particle. In brief, the heterogeneous strain field that appears around the tiled particles due to their complex morphology, is experimentally demonstrated by these pressure shadows. It is considered to be at the origin of the abrupt increase in the slope of $\gamma_T(L)$ at $L = b$ (Fig. 8a, cartoons and caption). It is also responsible for 'irregularities' in the rotation rates of the tiled objects when compared to the theoretical rates of simple-shaped objects.

DISCUSSION

Tiled crystals, mainly of K-feldspar and plagioclase, in a magma are generally considered to occur only within a dense suspension of crystals, i.e. when almost every crystal is in contact with its neighbours (Nicolas 1992, Tikoff & Teyssier 1994). If tiled crystals happen to form late in the crystallization history, and therefore magmatic deformation history, the whole grain fabric would also be concluded to be late magmatic. In support of this, it may be argued that, due to the absence of interactions between grains, grain shape fabrics at very high melt fractions should be erratic in D and α , and close to randomness on average if the model of Jeffery (1922) is applied to a variety of grain shape ratios.

This study shows that the concept of interaction-free fabric should be applied with caution since the tiling of particles is a process that takes place even in low-concentration suspensions. Tiled particles are transient features that form, disappear and are replaced by other patterns. The consequence of tiling for the shape fabrics seems to be fundamental since, as soon as a certain amount of shear strain is reached, it tends to stabilise α at values close to zero, or at slightly positive values (see Fig. 5c) due to the effect of β (Fig. 8), and to keep the magnitude of D at low values (see Fig. 5c). The main reason for this effect comes from the aspect ratios of the tiled particle aggregates which may be much higher than the particles themselves; therefore they have lower angular velocities, are more stable than the separate particles, and possibly less sensitive to any heterogeneity of the strain path (see Ildefonse *et al.* 1992b).

The definition of a low concentration suspension remains, however, imprecise. In terms of the probability of occurrence of interactions, the present study suggests that 2D concentrations of 13–14% appear to substantially affect the fabrics for $\gamma \geq 6$. For lower concentrations, the same effects would probably be observed, but

at larger γ values. It is also observed that, due to the aureole of perturbed flow around a particle, the frequency of interactions is more sensitive to the density of particles than to the area occupied by the particles. However, extrapolation to 3D remains an important, and as yet unsolved, question.

CONCLUSION

This study strengthens the argument that the statistical determination of tiling features in a magma is a good shear sense indicator. However, we are afraid that not many workers will be patient enough to use this criterion. Instead, due to the introduction of the β angle in the shape fabric, corresponding to the contribution of the tiled particles, we suggest that one should now look systematically to the asymmetry of the orientation distribution of the particles with respect to the shear plane. This approach, although based on a different analysis, has already been explored by Benn & Allard (1989) in gabbroic rocks, and by Launeau & Bouchez (1992) in granites.

The proposition that crystalline fabrics in magmas could be acquired relatively early, i.e. when the liquid fraction was still very high (say $\gg 50\%$), is an important result of the present study. Fabrics rapidly lose their cyclicity, consequently remain stable with positive α values whatever the strain intensity, and develop much lower D values than predicted from theory. As these features are characteristic of the fabrics of many plutons over huge areas (see Bouchez & Gleizes, 1995), it is tempting to deduce that common magmatic fabrics may be imprinted quite early with respect to the crystallization history of the magma. However, the earlier this magmatic fabric is acquired during emplacement, the more likely that it will be modified or destroyed by a subsequent shear regime. This is probably true so long as progressive syn-emplacement does not increase the suspension concentration sufficiently to freeze in the initial fabric. In such a case the initial fabric could only be overprinted by a strong post-emplacement solid state deformation. However, since the strain path during magma emplacement may vary significantly, the earlier the magmatic fabric is acquired, the more likely it may be modified or replaced by a new fabric imprinted at a lower liquid fraction. Rapid crystallization (i.e. high level emplacement and/or magma with a small temperature crystallization interval) would favour survival of an 'early' magmatic fabric. Hence, the overprint of an early fabric would be favoured by (1) slow crystallization or (2) strong post-emplacement solid state deformation.

Acknowledgements—This study is a part of the Doctorate thesis of Laurent Arbaret at the University of Clermont-Ferrand. The torsion apparatus was built at the University of Clermont-Ferrand. We thank Dimitrios Sokoutis and Neil Mancktelow for their constructive reviews of the manuscript and F. Barbecot for his active participation during the experiments. Financial support came from a MESR fellowship (L.A.) and URA CNRS no. 10 (Univ. Clermont-Ferrand) and no. 67 (Univ. Toulouse).

REFERENCES

- Benn, K. & Allard, B. 1989. Preferred mineral orientations related to magmatic flow in ophiolite layered gabbros. *J. Petrol.* **30**, 925–946.
- Blanchard, J.P., Boyer, P. & Gagny, C. 1979. Un nouveau critère de sens de mise en place dans une caisse filonienne: Le ôpincementô des minéraux aux épontes. *Tectonophysics* **53**, 1–25.
- Blumenfeld, P. 1983. Le ôtôilage des mégacristauxô, un critère d'écoulement rotationnel pour les fluidalités des roches magmatiques. Application au granite de Barbey-Sérôux (Vosges France). *Bull. Soc. géol. Fr.* **25**, 309–318.
- Blumenfeld, P. & Bouchez, J.L. 1988. Shear criteria in granite and migmatite deformed in the magmatic and solid states. *J. Struct. Geol.* **4**, 361–372.
- Bouchez, J.L. & Gleizes, G. 1995. Two-stage deformation of the Mont-Louis-Andorra granite pluton (Variscan Pyrenees) inferred from magnetic susceptibility anisotropy. *J. geol. Soc. Lond.* **152**, 669–679.
- Choukroune, P., Gapais, D. & Merle, O. 1987. Shear criteria and structural symmetry. *J. Struct. Geol.* **9**, 525–530.
- Den Tex, E. 1969. Origin of ultramafic rocks. Their tectonic setting and history. *Tectonophysics* **7**, 457–488.
- Fernandez, A., Febesse, J.L. & Mezure, J.F. 1983. Theoretical and experimental study of fabrics developed by different shaped markers in two-dimensional simple shear. *Bull. Soc. géol. Fr.* **7**, 319–326.
- Hanmer, S. 1990. Natural rotated inclusions in non-ideal shear. *Tectonophysics* **176**, 245–255.
- Ildefonse, B., Launeau, P., Bouchez, J.L. & Fernandez, A. 1992. Effect of mechanical interactions on the development of shape preferred orientations: a two dimensional experimental approach. *J. Struct. Geol.* **14**, 73–83.
- Ildefonse, B., Sokoutis, D. & Mancktelow, N.S. 1992. Mechanical interactions between rigid particles in a deforming ductile matrix. Analogue experiments in simple shear flow. *J. Struct. Geol.* **10**, 1253–1266.
- Ildefonse, B. & Mancktelow, N.S. 1993. Deformation around rigid particles: the influence of slip at the particle/matrix interface. *Tectonophysics* **221**, 345–359.
- Jeffery, G.B. 1922. The motion of ellipsoidal particles immersed in a viscous fluid. *Proc. Roy. Soc. Lond.* **102**, 201–211.
- Launeau, P. & Bouchez, J.L. 1992. Mode et orientation préférentielle de forme des granites par analyse d'images numériques. *Bull. Soc. géol. Fr.* **163**, 721–732.
- Nicolas, A. 1992. Kinematics in Magmatic Rocks with Special Reference to Gabbros. *J. Petrol.* **33**, 891–915.
- Passchier, C.W. & Simpson, C. 1986. Porphyroclast system as kinematic indicators. *J. Struct. Geol.* **8**, 831–843.
- Passchier, C.W. & Sokoutis, D. 1993. Experimental modelling of mantled porphyroclast. *J. Struct. Geol.* **15**, 895–909.
- Paterson, S.R., Vernon, R.H. & Tobisch, O.T. 1989. A review of criteria for the identification of magmatic and tectonic foliations in granitoids. *J. Struct. Geol.* **11**, 349–363.
- Tikoff, B. & Teyssier, C. 1994. Strain and fabric analyses based on porphyroclast interaction. *J. Struct. Geol.* **16**, 477–491.
- Van den Driessche, J. & Brun, J.P. 1987. Rolling structures at large shear strain. *J. Struct. Geol.* **9**, 691–704.
- Weijermars, R. 1986. Flow behaviour and physical chemistry of bouncing putties and related polymers in view of tectonic laboratory applications. *Tectonophysics* **124**, 325–358.
- Willis, D.G. 1977. A kinematic model of preferred orientation. *Bull. geol. Soc. Am.* **88**, 883–894.